

“Light-Cone” Dynamics After Quantum Quenches in Spin Chains

Lars Bonnes,^{1,*} Fabian H. L. Essler,² and Andreas M. Läuchli¹

¹*Institute for Theoretical Physics, University of Innsbruck, A-6020 Innsbruck, Austria*

²*The Rudolf Peierls Centre for Theoretical Physics, Oxford University, Oxford OX1 3NP, United Kingdom*

(Received 30 April 2014; revised manuscript received 10 September 2014; published 30 October 2014)

Signal propagation in the nonequilibrium evolution after quantum quenches has recently attracted much experimental and theoretical interest. A key question arising in this context is what principles, and which of the properties of the quench, determine the characteristic propagation velocity. Here we investigate such issues for a class of quench protocols in one of the central paradigms of interacting many-particle quantum systems, the spin-1/2 Heisenberg XXZ chain. We consider quenches from a variety of initial thermal density matrices to the same final Hamiltonian using matrix product state methods. The spreading velocities are observed to vary substantially with the initial density matrix. However, we achieve a striking data collapse when the spreading velocity is considered to be a function of the excess energy. Using the fact that the XXZ chain is integrable, we present an explanation of the observed velocities in terms of “excitations” in an appropriately defined generalized Gibbs ensemble.

DOI: 10.1103/PhysRevLett.113.187203

PACS numbers: 75.10.Jm, 02.30.Ik, 05.70.Ln

The last few years have witnessed a number of significant advances in understanding the nonequilibrium dynamics in isolated quantum systems. Much of this activity has focused on fundamental concepts such as thermalization [1–5] or the roles played by dimensionality and conservation laws [6–16].

Another key issue concerns the spreading of correlations out of equilibrium, and, in particular, the “light-cone” effect after global quantum quenches. The most commonly studied protocol in this context is to prepare the system in the ground state of a given Hamiltonian, and to then suddenly change a system parameter such as a magnetic field or interaction strength. At subsequent times the spreading of correlations can then be analyzed by considering the time dependence of two-point functions of local operators separated by a fixed distance. As shown by Lieb and Robinson [17,18], the velocity of information transfer in quantum systems is bounded. This gives rise to a causal structure in commutators of local operators at different times, although Schrödinger’s equation, unlike relativistic theories, has no built-in speed limit. Recently, the Lieb-Robinson bounds have been refined [19–21] and extended to mixed state dynamics in open quantum systems [21,22], as well as topological quantum order [23].

A striking consequence of the Lieb-Robinson bound is that the equal-time correlators after a quantum quench feature a light-cone effect [23], which is most pronounced for quenches to conformal field theories from initial density matrices with a finite correlation length [24]: connected correlations are initially absent, but exhibit a marked increase after a time $t_0 = x/2v$. This observation is explained by noting [25,26] that entangled pairs of quasiparticles initially located halfway between the two points of measurement propagate with the speed of light v

and, hence, induce correlations after a time t_0 . These predictions have been verified numerically in several systems, see, e.g., [27–32]. Very recently light-cone effects after quantum quenches have been observed in systems of ultracold atomic gases [33,34] and trapped ions [35,36]. The experimental work raises the poignant theoretical issue of which velocity underlies the observed light-cone effect in nonrelativistic systems at finite energy densities. Here there is no unique velocity of light, and quasiparticles in interacting systems will generally have finite lifetimes depending on the details of the initial density matrix.

In order to shed some light on this issue, we have carried out a systematic study of the spreading of correlations in the spin-1/2 Heisenberg XXZ chain, a key paradigm among interacting many-body quantum systems in one spatial dimension. We fix the final (quenched) Hamiltonian and vary the initial conditions over a large range of parameters. Moreover, we do not only consider initial pure states [29] but also prepare the system in thermal initial states as illustrated in Fig. 1(a). The latter is of significant interest in view of experimental realizations. Apart from a recent numerical study for local quenches [37], the spreading of signals in quenches from thermal states is basically unexplored.

Our numerical simulations are based on a quench extension of a recently proposed algorithm utilizing an optimized wave function ensemble called Minimally Entangled Typical Thermal States (METTS) [38,39] implemented within the matrix product state (MPS) framework. We come back to the description of the algorithm and a discussion of its performance towards the end of this Letter.

Results.—In the following we consider quenches to the spin-1/2 Heisenberg XXZ chain with anisotropy Δ ,

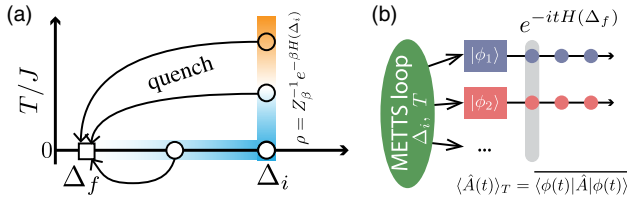


FIG. 1 (color online). (a) Quench protocol: The system is initially prepared in either the ground state of some Hamiltonian $H(\Delta_i)$ or in a thermal state $\rho = Z_\beta^{-1} \exp[-\beta H(\Delta_i)]$ with temperature T . At time 0, the anisotropy is quenched to Δ_f and we let the system evolve in time for various initial values of Δ_i and T . (b) Outline of the numerical procedure: The METTS projection loop generates an ensemble of wave function for some initial Δ_i and temperature T . Each realization is evolved in time and expectation values are obtained by averaging over the ensemble.

$$H(\Delta) = J \sum_{i=1}^{L-1} (S_i^x S_{i+1}^x + S_i^y S_{i+1}^y + \Delta S_i^z S_{i+1}^z). \quad (1)$$

Initially, the system is prepared in a Gibbs state corresponding to an XXZ Hamiltonian with anisotropy Δ_i at a temperature T , i.e., $\rho(t=0) = Z_\beta^{-1} \exp[-\beta H(\Delta_i)]$ with $\beta = 1/(k_B T)$, where $Z_\beta = \text{Tr} \exp[-\beta H(\Delta_i)]$ (we set $k_B = 1$). The anisotropy is then quenched at time $t = 0^+$ from Δ_i to $0 \leq \Delta_f \leq 1$, as depicted in Fig. 1(a), and the system subsequently evolves unitarily with Hamiltonian $H(\Delta_f)$ [40]. In order to probe the spreading of correlations we consider the longitudinal spin correlation functions $\mathcal{S}^z(j;t) = \langle S_{L/2}^z(t) S_j^z(t) \rangle - \langle S_{L/2}^z(t) \rangle \langle S_j^z(t) \rangle$ centered around the middle of the chain. Results for $\mathcal{S}^z(j;t)$ are most easily visualized in space-time plots, and typical results are shown in Fig. 2. The most striking feature observed in these plots is the light-cone effect: at a given separation j connected correlations $\mathcal{S}^z(j;t)$ arise fairly suddenly at a time that scales linearly with j .

These results demonstrate that the light-cone effect persists for mixed initial states, although the visibility of

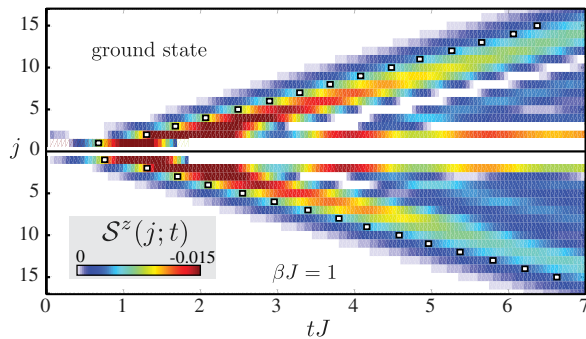


FIG. 2 (color online). Space-time plot of the \mathcal{S}^z correlation functions for the quench from $\Delta_i = 4$ to $\Delta_f = \cos(\pi/4)$. The upper panel shows ground state data whereas the lower panel shows data from a thermal density matrix at $T/J = 1$. This illustrates that the light-cone effect in this observable persists also at finite temperatures.

the signal is diminished with increasing temperature (until it vanished completely at $\beta = 0$, since the initial density matrix is trivial and stationary). Comparing the time evolution of the correlation functions for different initial temperatures, we see (cf. Figs. 2 and 3) that the signal front is delayed when the temperature of the initial state is increased, signaling that the spreading slows down. We further observe that the spreading velocity is sensitive to the strength of the quench, i.e., the value of the initial interaction. At this point we should note that this finding is unexpected. Based on our current understanding of quenches to CFTs or of Lieb-Robinson bounds, there are no predictions available which support spreading velocities depending on the initial state.

Having established the result that the spreading velocity depends both on the initial density matrices and the final Hamiltonian, an obvious question is which properties of $\rho(t=0)$ are relevant in this context. In order to quantify this aspect we define the precise location of the light cone as the first inflection point of the signal front observed in \mathcal{S}^z (also Ref. [29]). This allows us to extract a spreading velocity v_s by performing a linear fit to the largest accessible time, where expected finite-distance effects [41] are small.

Our main result, shown in Fig. 4, is that the spreading velocity is mainly determined by the final energy density $e_f = \text{Tr}[H(\Delta_f)\rho(t=0)]/L$. Plotting the measured velocities against e_f leads to a remarkable data collapse for a variety of quenches from thermal as well as pure initial states for various Δ_i . This holds in spite of the fact that the

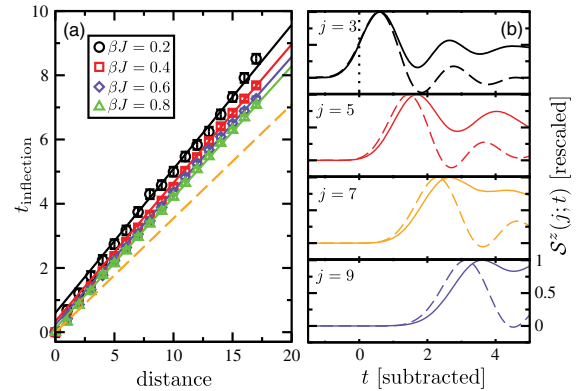


FIG. 3 (color online). (a) Extracted inflection points versus distance for different initial temperatures for the quench from $\Delta = 4$ to $\cos(\pi/4)$. The straight lines correspond to the velocities extracted from the GGE, where only the offset of the time axis has been fitted. The orange dashed line denotes the ground state Bethe ansatz velocity at Δ_f . (b) Rescaled averaged spin correlation functions for the quench from $\Delta = 4$ to $\cos(\pi/4)$ for $T/J = 1$ and the ground state (dashed line) and different distances $j = 3, 5, 7, \text{ and } 9$. We omit the error bars for clarity of the figure. The time axis is relative to the first inflection point of the correlation functions for $j = 3$. One can see that the signal is delayed as the initial temperature is increased.

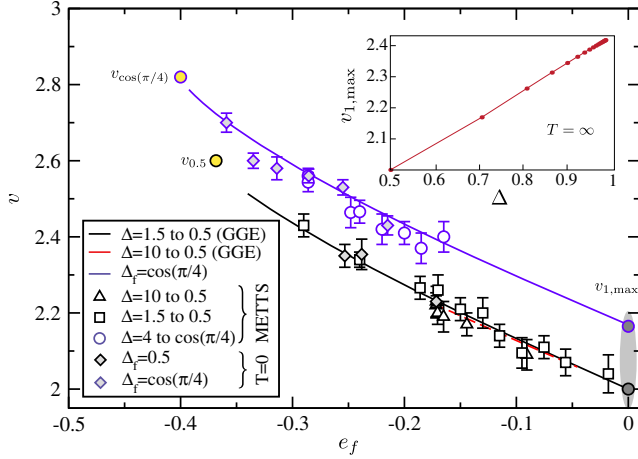


FIG. 4 (color online). Spreading velocity v_s extracted from the spin correlation function S^z as a function of the final energy e_f density for $\Delta_f = 1/2$ and $\cos \pi/4$. The symbols denote numerical results obtained from either thermal or pure initial states with different Δ_i . The blue and black solid lines denote the spreading velocities from TBA using only the energy density whereas the red line shows the results for the quench from $\Delta_i = 10$ to 0.5 using also the first conserved quantity. The corresponding velocities for the quench from $\Delta_i = 1.5$ lie on top of the black line; i.e., the GGE effects are smaller than the linewidth. The rightmost symbols denote v_{Δ_f} at the energy density of the ground state whereas the right most ones denote $v_{1,\max}$. The inset shows the velocity at $\beta = 0$, $v_{1,\max}$, extracted from the thermodynamic Bethe ansatz for $\Delta = \cos(\pi/n)$.

system is integrable and thus its dynamics is constrained by an infinite set of conserved quantities. As we will show in the following, the observed velocities can be explained quantitatively by considering excitations in an appropriately defined generalized Gibbs ensemble.

Focusing on the quenches to $\Delta_f = 1/2$ as well as $\cos(\pi/4) \approx 0.707$ [42], we observe that the spreading velocity v_s decreases significantly as the final energy density is increased by increasing T or altering Δ_i . The numerical data suggest that v_s approaches a nontrivial velocity in the infinite-temperature limit that depends on Δ_f . In fact, this velocity can be obtained from Bethe ansatz (see discussion below) and is shown for the series $\Delta_f = \cos(\pi/n)$ in the inset of Fig. 4. For very weak quenches, where only the low-energy [relative to the ground state of $H(\Delta_f)$] degrees of freedom become populated, one expects that the spreading velocity is given by the maximal mode velocity $v_{\Delta} = \pi[(1 - \Delta^2)/(2 \arccos \Delta)]^{-1/2}$. In fact, the spreading velocity extrapolates to v_{Δ_f} , when the final energy approaches the ground state energy of $H(\Delta_f)$. For the noninteracting case $\Delta_f = 0$ which reduces essentially to free fermions, we find that the spreading velocity for all initial conditions is compatible with the maximal mode velocity, $v_0 = 2$. This is consistent with results we obtained for quenches to the critical point of a one-dimensional Ising model in a transverse field, which is

essentially also a free theory, where also no significant dependence of the spreading velocity on the initial conditions was observed.

We now provide a theoretical explanation of our striking numerical observations.

Excitations in a generalized Gibbs ensemble.—A recent work [43] proposed that correlation functions of local operators after a quench to an integrable model, prepared in a pure state $|\Psi\rangle$, are given by

$$\lim_{L \rightarrow \infty} \langle \mathcal{O}(t) \rangle = \lim_{L \rightarrow \infty} \left[\frac{\langle \Psi | \mathcal{O}(t) | \Phi_s \rangle}{2 \langle \Psi | \Phi_s \rangle} + \Phi_s \leftrightarrow \Psi \right]. \quad (2)$$

Here, $|\Phi_s\rangle$ is a simultaneous eigenstate of the postquench Hamiltonian and all local, higher conservation laws I_n , such that

$$i_n \equiv \lim_{L \rightarrow \infty} \frac{1}{L} \text{Tr}[\rho(t=0) I_n] = \lim_{L \rightarrow \infty} \frac{1}{L} \frac{\langle \Phi_s | I_n | \Phi_s \rangle}{\langle \Phi_s | \Phi_s \rangle}. \quad (3)$$

In the case of interest here we have $\mathcal{O}(t) = S_{L/2}^z(t) S_j^z(t)$. Importantly, the state $|\Phi_s\rangle$ can be constructed by means of a generalized thermodynamic Bethe ansatz (gTBA) [44,45]. The stationary state itself is expected to be described by an appropriate GGE involving the known ultralocal [46] and quasiloca [47] conservation laws, and possibly others [48–52].

It was argued in Ref. [43] that states obtained by making microscopic changes to $|\Phi_s\rangle$ are most important to describe the dynamics at (sufficiently) late times. This is motivated by employing a Lehmann representation in terms of energy eigenstates $H(\Delta_f)|n\rangle = E_n|n\rangle$, $\langle \Psi | \mathcal{O}(t) | \Phi_s \rangle = \sum_n \langle \Psi | n \rangle \langle n | \mathcal{O} | \Phi_s \rangle \exp[-i(E_n - E_{\Phi_s})t]$, and noting that at sufficiently late times only states with $(E_n - E_{\Phi_s})/J = \mathcal{O}(1)$ are likely to contribute due to the otherwise rapidly oscillating phase. It is then tempting to conjecture that spreading of correlations occurs through these “excited states” (which by constructed can have either positive or negative energies relative to the representative state), and the light-cone effect propagates with the maximum group velocity that occurs amongst them. The method for calculating such excited state velocities is depicted schematically in Fig. 5, and details of the calculations are provided in the Supplemental Material [53]. The basic idea is to use TBA methods to determine the macrostate minimizing the generalized Gibbs free energy. This is characterized by appropriate particle-hole distribution functions $\rho_j^{p,h}(x)$ for elementary excitations labeled by the index j (x parametrizes the respective momenta). The corresponding “microcanonical” description [43,57,58] is based on the particular simultaneous eigenstate $|\Phi_s\rangle$ of the Hamiltonian and the higher conservation laws, characterized by the set $\{\rho_j^{p,h}(x)\}$ in the thermodynamic limit. One then considers small changes of this microstate, and

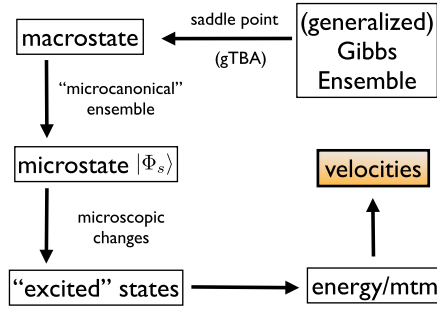


FIG. 5 (color online). Scheme for the extraction of the velocities from the GGE. See text for details.

determines the resulting $\mathcal{O}(1)$ (i.e., nonextensive) changes in energy and momentum. These can be described in terms of additive “elementary excitations” relative to $|\Phi_s\rangle$. Finally, one determines the dispersion relations and hence the group velocities of these excitations. The most significant qualitative features of the “GGE excitation spectrum” obtained in this way are as follows. (i) There are several types of infinitely long-lived elementary excitations. (ii) Their number depends only on the anisotropy Δ_f [59], but their dispersions are sensitive to the full set $\{i_n\}$ of (conserved) expectation values. (iii) In practice, we need to compute i_n numerically. Given that explicit expressions for I_n become rapidly extremely complicated [46], we retain only two conservation laws, namely, energy and I_3 , which involves 4-spin interactions (I_2 is odd under time reversal and hence does not play a role for the quenches considered here). This can be justified by noting that the differences in the calculated maximal velocities between a Gibbs ensemble and a GGE with one added conservation law are small, and that the most local conservation laws are most important for accurately describing the properties of local operators [60]. (iv) In the cases we have considered, the maximal propagation velocity is found for the same type of excitation (“positive parity 1 strings” [59]). The results for the maximal velocities obtained from this gTBA analysis are compared to our numerical computations in the main panel of Fig. 4. The agreement is clearly very good. Also, the inset of Fig. 4 shows the velocities for infinite temperatures ($e_f = 0$) for $\Delta_f = \cos(\pi/n)$, where n is an integer, revealing a non-trivial Δ_f dependence even in this limiting case.

Numerical method.—After having provided the physical results we shortly review the numerical procedure employed to simulate the mixed state dynamics. MPS provide a powerful framework to study the real-time dynamics of one-dimensional quantum systems. Originally conceived for ground state calculations [61], there exist various extensions to finite temperatures [62–72]. Very recently, Refs. [38,39] introduced a stochastic method in which the expectation value of a thermal density matrix is replaced by an average over an ensemble

of wave functions $\{|\phi_i\rangle\}$, that (i) can be efficiently sampled (importance sampling) using Markov chains and (ii) only hosts the minimal (small) amount of entanglement required at that temperature, thus allowing for an efficient representation in terms of MPS and was therefore called METTS.

We show that the METTS method, thus far only applied to static equilibrium problems, can be easily extended to study real time evolution by realizing that the expectation value of some real-time propagated operator $\hat{A}(t)$ can be written as $\langle \hat{A}(t) \rangle_T = 1/Z_\beta \text{Tr} \exp(-\beta H) \hat{A}(t) = \overline{\langle \phi_i(t) | \hat{A} | \phi_i(t) \rangle}$, where the last term denotes an average over the time-evolved METTS ensemble [73]. We employ the numerical scheme illustrated in Fig. 1(b) where we first generate an ensemble of wave functions following Ref. [39]. In a second step each Φ_i is evolved in time using the TEBD algorithm [61] and $\langle \hat{A}(t) \rangle_T$ is evaluated. We average over a few hundred METTS instances and are limited due to runaway phenomena [74] to times of $tJ \sim 6-8$. Because of the reachable time scales we consider system sizes of up to 50 sites here, but studying larger systems poses no particular problem by itself. A detailed description of the numerical method used here can be found in the Supplemental Material [53].

Compared to a complementary approach, where the von Neumann equation for the full system density matrix is integrated within an matrix product operator framework [67], we find that the METTS approach is able to reach significantly longer times, and we therefore believe that the METTS approach is quite promising to study global quenches at finite temperature. A full comparison of the different approaches, however, is beyond the scope of this Letter and will be addressed in a forthcoming publication [75].

Conclusions.—We have analyzed the spreading of correlations after quantum quenches in the spin-1/2 Heisenberg XXZ chain. Our initial density matrix describing the system was taken to be a Gibbs distribution at a particular temperature and initial value of anisotropy Δ_f . We observed a pronounced light-cone effect in the connected longitudinal spin-spin correlation function. We found that the propagation velocity v of the light-cone depends not only on the final Hamiltonian, but also on the initial density matrix. For the quenches we considered the observed values of v are well characterized by the expectation value of the final Hamiltonian in the initial state. These findings were found to be in accord with expectation based on properties of excitations in an appropriately defined generalized Gibbs ensemble. We also have shown that one can apply the METTS framework to study dynamical properties using MPS. Although the method also exhibits the typical runaway behavior, the lack of ancillary degrees of freedom or enlarged local Hilbert spaces reduces the complexity of the simulations and a direct comparison to other methods will be provided in a separate publication [75].

Our work raises a number of interesting issues. First, we expect that a full characterization of v will involve not only the final energy density, but the densities of all final higher conservation laws as well. In fact, we observe that the effects of higher conserved quantities are much more pronounced for negative Δ_f and this point is under investigation. Second, our work raises the question, whether horizon effects related to slower excitations can become visible for particular initial density matrices (in the case of local quenches this is indeed the case [76]). Finally, our work suggests that light-cone propagation in generic nonintegrable models ought to be rather nontrivial and warrants detailed investigation.

We thank S. R. Manmana for discussions and acknowledge R. Bartenstein for collaboration at an early stage of the project. This work was supported by the Austrian Ministry of Science BMWF as part of the UniInfrastrukturprogramm of the Forschungsplattform Scientific Computing at LFU Innsbruck, by the Austrian Science Fund (FWF) through the SFB FoQuS (FWF Project No. F4018-N23) and by the EPSRC under Grants No. EP/I032487/1 and No. EP/J014885/1.

*lars.bonnes@uibk.ac.at

- [1] M. Rigol, V. Dunjko, and M. Olshanii, *Nature (London)* **452**, 854 (2008).
- [2] J. M. Deutsch, *Phys. Rev. A* **43**, 2046 (1991).
- [3] M. Srednicki, *Phys. Rev. E* **50**, 888 (1994).
- [4] M. Srednicki, *J. Phys. A* **29**, L75 (1996).
- [5] M. Srednicki, *J. Phys. A* **32**, 1163 (1999).
- [6] M. Rigol, V. Dunjko, V. Yurovsky, and M. Olshanii, *Phys. Rev. Lett.* **98**, 050405 (2007).
- [7] A. Iucci and M. A. Cazalilla, *Phys. Rev. A* **80**, 063619 (2009).
- [8] P. Calabrese, F. H. L. Essler, and M. Fagotti, *J. Stat. Mech.: Theory Exp.* (2012) P07016.
- [9] T. Barthel and U. Schollwöck, *Phys. Rev. Lett.* **100**, 100601 (2008).
- [10] M. Cramer, C. M. Dawson, J. Eisert, and T. J. Osborne, *Phys. Rev. Lett.* **100**, 030602 (2008).
- [11] M. Cramer and J. Eisert, *New J. Phys.* **12**, 055020 (2010).
- [12] D. Fioretto and G. Mussardo, *New J. Phys.* **12**, 055015 (2010).
- [13] P. Calabrese, F. H. L. Essler, and M. Fagotti, *Phys. Rev. Lett.* **106**, 227203 (2011).
- [14] P. Calabrese, F. H. L. Essler, and M. Fagotti, *J. Stat. Mech.: Theory Exp.* (2012) P07022.
- [15] J.-S. Caux and R. M. Konik, *Phys. Rev. Lett.* **109**, 175301 (2012).
- [16] M. Collura, S. Sotiriadis, and P. Calabrese, *Phys. Rev. Lett.* **110**, 245301 (2013).
- [17] E. H. Lieb and D. W. Robinson, *Commun. Math. Phys.* **28**, 251 (1972).
- [18] R. Sims and B. Nachtergaele, *Lieb-Robinson Bounds in Quantum Many-Body Physics*, edited by R. Sims and D. Ueltschi, Entropy and the Quantum, Vol. 529 (American Mathematical Society, Providence, RI, 2010).
- [19] J. Jünemann, A. Cadarso, D. Perez-Garcia, A. Bermudez, and J. J. Garcia-Ripoll, *Phys. Rev. Lett.* **111**, 230404 (2013).
- [20] E. H. Lieb and A. Vershynina, [arXiv:1306.0546v1](https://arxiv.org/abs/1306.0546v1).
- [21] M. Kliesch, C. Gogolin, and J. Eisert, *Lieb-Robinson Bounds and the Simulation of Time Evolution of Local Observables in Lattice Systems*, edited by L. D. Site and Bach, Many-Electron Approaches in Physics, Chemistry and Mathematics: A Multidisciplinary View (Springer, New York, 2013).
- [22] D. Poulin, *Phys. Rev. Lett.* **104**, 190401 (2010).
- [23] S. Bravyi, M. B. Hastings, and F. Verstraete, *Phys. Rev. Lett.* **97**, 050401 (2006).
- [24] P. Calabrese and J. Cardy, *Phys. Rev. Lett.* **96**, 136801 (2006).
- [25] P. Calabrese and J. Cardy, *J. Stat. Mech.: Theory Exp.* (2005) P04010.
- [26] P. Calabrese and J. Cardy, *J. Stat. Mech.: Theory Exp.* (2007) P06008.
- [27] G. De Chiara, S. Montangero, P. Calabrese, and R. Fazio, *J. Stat. Mech.: Theory Exp.* (2006) P03001.
- [28] A. M. Läuchli and C. Kollath, *J. Stat. Mech.: Theory Exp.* (2008) P05018.
- [29] S. R. Manmana, S. Wessel, R. M. Noack, and A. Muramatsu, *Phys. Rev. B* **79**, 155104 (2009).
- [30] P. Hauke and L. Tagliacozzo, *Phys. Rev. Lett.* **111**, 207202 (2013).
- [31] J. Eisert, M. van den Worm, S. R. Manmana, and M. Kastner, *Phys. Rev. Lett.* **111**, 260401 (2013).
- [32] G. Carleo, F. Becca, L. Sanchez-Palencia, S. Sorella, and M. Fabrizio, *Phys. Rev. A* **89**, 031602 (2014).
- [33] M. Cheneau, P. Barmettler, D. Poletti, H. Endres, P. Schauß, T. Fukuhura, C. Gross, I. Bloch, C. Kollath, and S. Kuhr, *Nature (London)* **481**, 484 (2012).
- [34] T. Langen, R. Geiger, M. Kuhnert, B. Rauer, and J. Schmiedmayer, *Nat. Phys.* **9**, 640 (2013).
- [35] P. Jurcevic, B. P. Lanyon, P. Hauke, C. Hempel, P. Zoller, R. Blatt, and C. F. Roos, *Nature (London)* **511**, 202 (2014).
- [36] P. Richerme, Z.-X. Gong, A. Lee, C. Senko, J. Smith, M. Moss-Feig, S. Michalakis, A. V. Gorshkov, and C. Monroe, *Nature (London)* **511**, 198 (2014).
- [37] C. Karrasch, J. E. Moore, and F. Heidrich-Meisner, *Phys. Rev. B* **89**, 075139 (2014).
- [38] S. R. White, *Phys. Rev. Lett.* **102**, 190601 (2009).
- [39] E. M. Stoudenmire and S. R. White, *New J. Phys.* **12**, 055026 (2010).
- [40] Note that the system is not connected to a heat bath during the time evolution and energy $\text{Tr}[H\rho(t)]$ is conserved.
- [41] P. Barmettler, D. Poletti, M. Cheneau, and C. Kollath, *Phys. Rev. A* **85**, 053625 (2012).
- [42] This particular value of the final interaction, $\Delta_f = \cos(\pi/n)$ is chosen due to technical reasons in the Bethe ansatz calculations.
- [43] J.-S. Caux and F. H. L. Essler, *Phys. Rev. Lett.* **110**, 257203 (2013).
- [44] J. Mossel and J.-S. Caux, *J. Phys. A* **45**, 255001 (2012).
- [45] E. Demler and A. M. Tsvelik, *Phys. Rev. B* **86**, 115448 (2012).
- [46] M. P. Grabowski and P. Mathieu, *Ann. Phys. (N.Y.)* **243**, 299 (1995).
- [47] T. Prosen and E. Ilievski, *Phys. Rev. Lett.* **111**, 057203 (2013).

- [48] B. Pozsgay, *J. Stat. Mech.: Theory Exp.* **(2013)** P07003.
- [49] M. Fagotti and F. H. L. Essler, *J. Stat. Mech.: Theory Exp.* **(2013)** P07012.
- [50] M. Fagotti, M. Collura, F. H. L. Essler, and P. Calabrese, *Phys. Rev. B* **89**, 125101 (2014).
- [51] B. Wouters, M. Brockmann, J. De Nardis, D. Fioretto, and J.-S. Caux, *Phys. Rev. Lett.* **113**, 117202 (2014).
- [52] B. Pozsgay, M. Mestyán, M. A. Werner, M. Kormos, G. Zaránd, and G. Takás, *Phys. Rev. Lett.* **113**, 117203 (2014).
- [53] See Supplemental Material at <http://link.aps.org/supplemental/10.1103/PhysRevLett.113.187203>, which includes Refs. [54–56].
- [54] V. E. Korepin, A. G. Izergin, and N. M. Bogoliubov, *Quantum Inverse Scattering Method, Correlation Functions and Algebraic Bethe Ansatz* (Cambridge University Press, Cambridge, England, 1993).
- [55] M. Takahashi, *Thermodynamics of One-Dimensional Solvable Models* (Cambridge University Press, Cambridge, England, 1999).
- [56] N. Muramoto and M. Takahashi, *J. Phys. Soc. Jpn.* **68**, 2098 (1999).
- [57] B. Pozsgay, *J. Stat. Mech.* (2011) P01011.
- [58] A. C. Cassidy, C. W. Clark, and M. Rigol, *Phys. Rev. Lett.* **106**, 140405 (2011).
- [59] M. Takahashi and M. Suzuki, *Prog. Theor. Phys.* **48**, 2187 (1972).
- [60] M. Fagotti and F. H. L. Essler, *Phys. Rev. B* **87**, 245107 (2013).
- [61] G. Vidal, *Phys. Rev. Lett.* **91**, 147902 (2003).
- [62] A. E. Feiguin and S. R. White, *Phys. Rev. B* **72**, 220401 (2005).
- [63] T. Barthel, U. Schollwöck, and S. R. White, *Phys. Rev. B* **79**, 245101 (2009).
- [64] C. Karrasch, J. H. Bardarson, and J. E. Moore, *Phys. Rev. Lett.* **108**, 227206 (2012).
- [65] T. Barthel, *New J. Phys.* **15**, 073010 (2013).
- [66] C. Karrasch, J. H. Bardarson, and J. E. Moore, *New J. Phys.* **15**, 083031 (2013).
- [67] M. Zwolak and G. Vidal, *Phys. Rev. Lett.* **93**, 207205 (2004).
- [68] F. Verstraete, J. J. Garcia-Ripoll, and J. I. Cirac, *Phys. Rev. Lett.* **93**, 207204 (2004).
- [69] T. Prosen and M. Žnidarič, *J. Stat. Mech.: Theory Exp.* **(2010)** P07020.
- [70] R. J. Bursill, T. Xiang, and G. A. Gehring, *J. Phys. Condens. Matter* **8**, L583 (1996).
- [71] X. Wang and T. Xiang, *Phys. Rev. B* **56**, 5061 (1997).
- [72] J. Sirker and A. Klümper, *Phys. Rev. B* **71**, 241101 (2005).
- [73] It is possible to evaluate observables that commute with the projection operator using the CPS rather than the METTS. The real time evolution, though, prohibits us from taking advantage of this improved measurement scheme.
- [74] D. Gobert, C. Kollath, U. Schollwöck, and G. Schütz, *Phys. Rev. E* **71**, 036102 (2005).
- [75] L. Bonnes and A. M. Läuchli (to be published).
- [76] M. Ganahl, E. Rabel, F. H. L. Essler, and H. G. Evertz, *Phys. Rev. Lett.* **108**, 077206 (2012).